Computer Networks and Communications
http://ojs.wiserpub.com/index.php/CNC/

Research Article

Energy Consumption Model for Full-Duplex LoRa Backscatter-Based Sensor Node

Siaka Konaté[1,2*], Changli Li[3], Drissa Traoré[1], Diouba Sacko[4], Souleymane Coulibaly[5]

[1] Department of Electronic, Normal School of Technical and Vocational Education, Bamako, Mali
[2] School of Information and Communication Engineering, Hohai University, Nanjing, China
[3] School of Artificial Intelligence, Nanjing University of Information Science and Technology, Nanjing, China
[4] Department of Electronic, National School for Engineering (ENI-ABT), Bamako, Mali
[5] Department of Energy, Normal School of Technical and Vocational Education, Bamako, Mali
[*] Correspondence: konatesiaka77@gmail.com

Received: 19 May 2026; **Revised:** 21 June 2026; **Accepted:** 29 June 2026; **Published:** 17 August 2026

Abstract: The integration of Wireless Sensor Networks (WSNs) into Internet of Things (IoT) brings new challenges in terms of range and energy consumption. Specifically, energy consumption is of great importance for future IoT sensors. Therefore, a thorough study must be performed to understand and evaluate the impact of different parameters that affect sensor node energy consumption. However, LoRa backscatter has been seen as a promising technology for long-range low-power IoT applications. Hence, this paper addresses the modeling of the energy consumption of a LoRa backscatter-based sensor node. We first derive the energy model for single-node communication and extend it to multiple-sensor-node communication where several sensors concurrently transmit their information. Furthermore, we derive an energy model for a battery-free sensor node that relies on the energy harvested from ambient sources to drive its operation. The simulation results show that both the LoRa parameters (such as payload size), the number of nodes in the network, and the number of retransmissions can impact the total energy consumption of the sensor node. Additionally, a single node powered by a battery with a capacity of 225 mAh and a transmission of 20 bytes every 5 minutes has a lifetime of about 14 years.

***Keywords*:** LoRa backscatter, energy consumption, low power communication, Internet of Things (IoT), Wireless Sensor Networks (WSNs)

1. Introduction

The rapid development of Internet of Things (IoT) has facilitated the integration of Wireless Sensor Networks (WSNs) with Internet connectivity. IoT devices are expected to reach more than 75 billion worldwide by 2025 [1]. This integration allows for a wide variety of applications, including home, industrial, healthcare, and environmental [2]. The incorporation of WSNs into IoT brings new challenges in terms of data acquisition, energy consumption, range, and energy harvesting [3].

To achieve long-range communication with minimal power consumption, many research studies have been conducted on communication protocols that meet these requirements. Among Low-power communication technologies, LoRa

Copyright ©2026 Siaka Konaté, et al.
DOI: https://doi.org/10.37256/cnc.42202610179
This is an open-access article distributed under a CC BY license
(Creative Commons Attribution 4.0 International License)
https://creativecommons.org/licenses/by/4.0/

backscatter seems to be a promising solution for long-range low-power IoT applications. This solution has been broadly addressed in the literature to validate use cases. In the literature, a wide variety of potential IoT applications have been proposed for LoRa backscatter in fields such as health monitoring, environmental monitoring, security, and localization [4–11]. The works in [6, 12–18] address LoRa backscatter tag designs. The error performance of LoRa backscatter systems is analyzed in [19–21]. The energy consumption model is not adequately addressed in the literature. Some works have simply reported the power consumption data of the LoRa backscatter tag in their experiments [6, 12, 14–16, 18] using proof-of-concept prototypes.

In this paper, we propose a novel, more accurate, and up-to-date energy consumption model for LoRa backscatter technology. The key contributions of this paper are as follows. First, we present an up-to-date energy consumption model that characterizes the current consumption and lifetime of a LoRa backscatter-based sensor node. Second, we extend the model to evaluate the impact of collisions and transmission errors on total energy consumption. The effects of parameters such as the number of sensors in the network, the number of retransmissions, and the size of the tag payload are also analyzed. Finally, the energy consumption model for a node powered by ambient energy is proposed for battery-free IoT device communication.

The remainder of this work is organized as follows. The Section 2 presents related works. Section 3 presents an overview of the LoRa/LoRaWAN technology. The principle of LoRa backscatter is presented in Section 4. We present our sensor node design in Section 5. The energy consumption model is presented in Section 6. The Section 7 presents the simulation results and discussion. Finally, the conclusion and future research directions are given in Section 10.

2. Related works

As a low-power technology, it is crucial to investigate its energy characteristics. Only a few works address this issue. The LoRaWAN energy consumption model is developed in [22] to characterize the current consumption of the LoRaWAN end-device, the lifetime, and the energy cost of data delivery. The proposed model is based on measurements performed on a currently prevalent LoRaWAN platform. The authors derived two separate models: the first for unacknowledged transmission and the second for acknowledged transmission. In addition, they extend the model to evaluate the impact of packet loss due to packet loss. However, their proposal is based on a single-node energy model, and the network density can affect the energy consumption of the LoRaWAN network. In [23], a refined node energy consumption model is presented for the LoRaWAN network. This improved model takes into account the number of nodes in the network, the collision probability that depends on the density of the sensors, and the number of retransmissions. However, it is only used for active LoRa technology. The above works propose energy consumption models for active wireless communication technologies to quantify the impact of various system parameters on the energy consumption and lifetime of sensor nodes. However, these models are not directly applicable to LoRa backscatter technology because they do not capture its unique communication characteristics and energy consumption mechanisms. Consequently, they do not accurately represent the energy consumption behavior of LoRa backscatter-based sensor nodes.

In this work, we propose an improved energy consumption model for LoRa backscatter-based sensor nodes that will be used to compute the battery lifetime of sensor nodes communicating using LoRa backscatter. The proposed energy model takes into account the different states traversed by the end device for both uplink and downlink transmissions. The effects of collisions, transmission errors, and the number of nodes in the network are all considered in the proposed energy model. We also propose an energy harvesting model for non-battery-operated sensor nodes.

3. LoRa/LoRaWAN basic

LoRa backscatter communication is based on LoRa/LoRaWAN technology, which is a proprietary spread spectrum modulation scheme based on chirp spread modulation (CSS) [24] developed by Cycleo, a French Tech company, later acquired by Semtech. LoRaWAN is the underlying technology (protocols) developed by the LoRa Alliance, a group of the most influential companies in the global telecommunications industry, including but not limited to IBM, Semtech, and

HP [25] to name a few, whose mission is to achieve Massive IoT through the global adoption of LoRaWAN technology. LoRa uses six spreading factors (SF7 to SF12) in the scheme to adapt the data rate and coverage range, link robustness, or energy consumption tradeoff. A higher spreading factor allows for a longer range at the expense of a lower data rate, and vise versa [26]. LoRa operates in three ISM bands: 433 MHz (Europe), 915 MHz (North America), and 433 MHz (Asia). To improve robustness and protect the transmitted signal from error bursts, LoRa employs a forward error correction utilizing four sets of coding rates (CR) from 1 to 4. A higher coding rate results in a more reliable link to interference, but at the price of a longer packet time on air (ToA) [27].

The main characteristics of LoRa and LoRaWAN are summarized in Table 1.

Table 1. LoRa main features

Features	LoRa
Modulation	CSS
Operating frequency	Unlicensed ISM bands (868 MHz in Europe, 915 MHz in North America, and 433 MHz in Asia)
Bandwidth	125 kHz, 250 kHz and 500 KHz
Data rate	0.3 to 50 kbps
Spreading factor (SF)	From SF7 to SF12
Coding rate (CR)	From 4/5 to 4/8
Transmission mode	Bidirectional half duplex
Duty cycle	1% or 0.1%
Maximum messages per day	Unlimited
Maximum payload length	243 bytes
Range	5 km (urban), 20 km (rural)
Authentication and encryption	AES 128b

The LoRa packet comprises three elements: the preamble, header (optional), and payload, as shown in Figure 1. The preamble is used to detect the start of the packet by the receiver. The header provides information on the payload, such as the payload length in bytes, the forward error correction code rate, and the presence of an optional 16-bit CRC for the payload. The payload is a variable-length field that contains the actual data encoded at the forward error correction code rate, either as specified in the header in explicit mode or fixed in implicit mode. An optional payload CRC may be included.

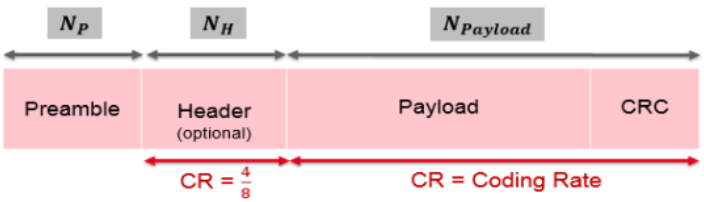


Figure 1. LoRa packet structure

4. LoRa backscatter systems

4.1 *Link budget*

The signal received from the bistatic systems is calculated as [28]

$$P_R = \frac{P_t G_T G_R G_t^2 X_b X_f \sigma}{B_b B_f \theta F_\beta} \left(\frac{\lambda}{4\pi}\right)^4 \frac{1}{(d_1 d_2)^n}. \tag{1}$$

Where X_f and X_b are the polarization mismatches of the forward and backward links, respectively. B_f and B_b are the forward and backward lint path blockages, respectively. σ is the modulation factor (tag reflection efficiency). θ is the RF tag antenna's on-object gain penalty, and F_β is the small-scale fading loss for a bistatic dislocated backscatter configuration.

We assume P_R to be the receiver sensitivity of the LoRa receiver (Gateway) that presents the minimum received power to detect the signal. The sensitivity is determined for the minimum signal-to-noise ratio denoted $\frac{E_b}{N_0}$ as [29]:

$$P_R = \frac{E_b}{N \cdot N_0} \cdot K \cdot T \cdot BW \cdot NF \tag{2}$$

where K, T, BW, and NF are Boltzmann's constant, the temperature, the bandwidth, and the noise figure, respectively. The value of K is equal to 1.38×10^{-23} W/Kelvin · Hz.

From equation (2), we define $\frac{E_b}{N_0}$ in decibels as:

$$\frac{E_b}{N_0} = P_R(dB) - 10log(KT) - NF(dB) - 10log(\frac{B}{2^{SF}}) \tag{3}$$

where $\frac{B}{2^{SF}}$ corresponds to the symbol rate.

5. Sensor node design

The proposed LoRa backscatter-based sensor node model is shown in Figure 2. It comprises a controller, a modulator, a demodulator, sensing devices, and a power harvesting module. The power harvesting module includes the RF harvester, the supercapacitor, and the power management unit.

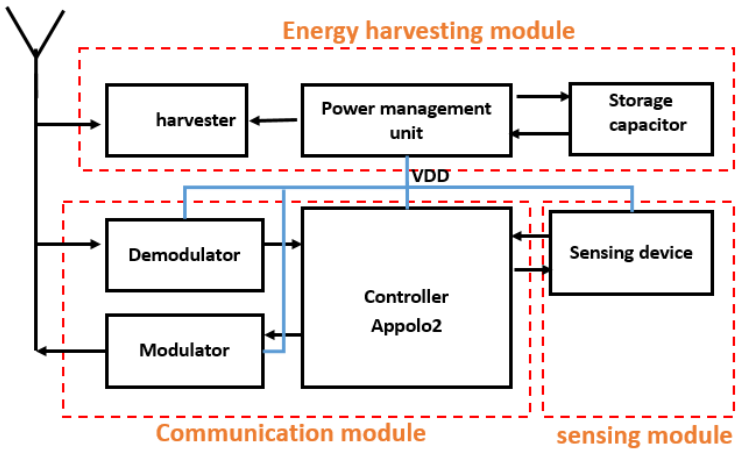


Figure 2. Proposed LoRa backscatter-based sensor node architecture

We consider a sensor network where each device transmits its measured data using LoRa backscatter communication. Sensor nodes measure soil moisture and temperature values in an irrigation field, and a microcontroller is used to process the measured data and backscatter it to a LoRa receiver, as shown in Figure 3. A user accesses the sensor readings and controls the field remotely using an electronic device.

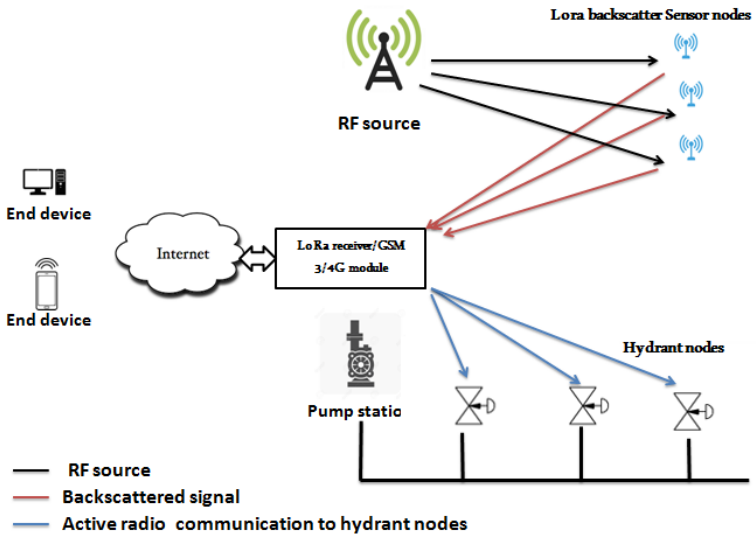


Figure 3. Architecture of smart agriculture systems

The sensor node comprises three main units: the energy harvesting module, the sensing devices, and the communication module.

The sensor operates in three distinct modes, i.e., harvesting mode, transmission mode, and reception mode. In harvesting mode,the received energy from the antenna is converted into DC power and stored in a capacitor to power the sensor node. When the sensor needs to transmit data, it detects the presence of a LoRa symbol using a preamble detection circuit and maps its data onto it. Finally, in reception mode,the sensor node synchronizes with the preamble and starts decoding the encoded LoRa backscatter data.

5.1 *Processing unit*

The processing unit is the main component of the sensor node. It is used for different tasks, such as reading the sensor unit's measured data and processing all the commands to and from the other peripherals and components in the sensor board. The power consumption of the processing unit has a direct impact on the total energy consumption of the node. Therefore, it must be chosen for low power consumption. In the paper, we use the Appollo2 [30] low-power microcontroller from ambiqmicro as a processing unit, which has a power consumption of 10 μW/MHz. This indicates that higher clock speeds result in higher power consumption.

5.2 *Sensing device*

A sensor is an electronic device that is used to measure a change in the environment. It measures a physical quantity and converts it into an electric signal. Here, we use an SHTC3 temperature and humidity sensor [31] from SENSIRION company for data measurement, which consumes about 270 μW.

5.3 *Packet detection module*

The packet detector exploits the unique structure of the LoRa preamble to detect the presence of an incoming LoRa signal and synchronize with it to backscatter tag data. The preamble detector is characterized by its sensitivity and power consumption. We use the packet detector in [16], which consumes about 93.2 μW.

5.4 *Backscatter modulator*

The backscatter modulation consists of varying the impedance value of an RF switch using the baseband signal generated by the microcontroller. The modulation part is based on the Apollo2 microcontroller (the one used to process the sensing data) and the reflective RF switch ADG902 [32], which has a current consumption of approximately 1 μA.

6. The proposed energy consumption model

The proposed energy model is divided into three parts. First, the energy consumption of a single device operating on a battery and transmitting using LoRa backscatter is developed. We assume that there is no error during a single-device transmission. Therefore, the probability of error is zero. Second, we extend the model to multiple device transmission cases that are subject to collisions and transmission errors, resulting in data retransmissions. Finally, we consider the scenario where the sensor nodes are battery-free and energy is extracted from ambient sources.

6.1 *Single device energy model*

We propose a simple energy model that considers all the energy components contributing to the overall energy consumption during the active mode. Primarily, we average the current consumption of a single battery-operated LoRa backscatter-based node that transmits data denoted as I_{av_s}. To determine this parameter, we first derive a profile of the different states traversed by the device, as well as the duration and current consumed in each state. We assume a cyclic transmission, as shown in Figure 4, where the device performs all tasks and repeats the process periodically. We model the current consumption during one cycle.

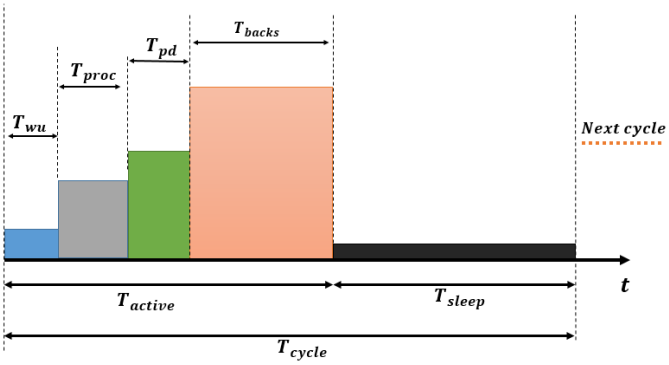


Figure 4. Sensor node working states illustration for uplink transmission

Each cycle comprises the related states involved in the data transmission of the LoRa backscatter device. The Table 2 presents the different states involved in one cycle of sensor node operation. The device is put in sleep mode at the end of each cycle to save energy. The total current consumption is given as:

$$I_{total} = I_{active} + I_{sleep} \tag{4}$$

where I_{active} and I_{sleep} are the current consumptions during active and sleep modes, respectively. The current consumption during the active state is given as

$$I_{active} = \sum_{i=1}^{N} I_i = I_{active} = I_{wu} + I_s + I_{proc} + I_{pd} + I_{backs}. \tag{5}$$

Where I_{proc} is the current consumption of the microcontroller for data processing, I_{wu} is the current consumption during the wake-up state, I_{pd} is the current consumption of the preamble detector, I_s is the current consumed by the sensing devices, and I_{backs} is the current consumption during the backscatter transmission state. The wake-up of the sensor node is managed by the microcontroller. Therefore, The current consumption during the wake-up state depends on the microcontroller.

Table 2. Different states in single battery-operated LoRa backscatter node communication with their duration and current consumption

States	Description	Duration		Current consumption	
		Variable	Values	Variable	Values
1	Wake up	T_{wu}	15us	I_{wu}	10 μA/MHz [30]
2	sensing	T_s	0.7ms	I_s	270 μA [31]
3	processing	T_{proc}	4ms	I_{proc}	10 μA/MHz [30]
4	preamble detection	T_{pd}	Equation (10)	I_{pd}	93.2 μW [16]
5	backscatter	T_{backs}	Equation (11)	I_{backs}	Equation (6)
6	Sleep	I_{sleep}	Equation (8)	I_{sleep}	2.9 uA [30]

During the backscatter transmission state, the microcontroller is used to generate the baseband modulated signal. Next, an RF front-end executes the backscatter operation that encapsulates the modulated information into the LoRa carrier received from the gateway and scatters it back to the receiver. Therefore, the total current consumption of the backscatter transmitter is the summation of the current consumption of the Microcontroller Unit (MCU) for baseband processing and the current consumption of the Rf switch for the backscatter operation and is given as:

$$I_{backs} = I_{MCU} + I_{sw} \tag{6}$$

where I_{MCU} is the current consumed by the microcontroller for baseband generation and I_{sw} is the current consumed by the RF switch. The total energy consumption during the backscatter operation is mainly dependent on the power consumption of the microcontroller, which varies with the switching frequency during data modulation. For example, the authors in [33] use a low-power MSP430 microcontroller [34], which has a power consumption of 7.2 mW to reduce the overall power consumption of the backscatter transmitter.

Let T_i and I_i denote the duration and current consumption of state I in Table 2. The average current consumption can then be calculated as

$$I_{av_s} = \frac{1}{T_{cycle}} \sum_{i=1}^{N} T_i I_i \tag{7}$$

where N is the number of states involved in the sensor operation and T_{cycle} is the duration of one cycle of sensor node operation. Sleep time T_{sleep} can be calculated as:

$$T_{sleep} = T_{cycle} - T_{active}. \tag{8}$$

Where T_{active} denotes the sum of the durations of all states related to sensor node operation in active mode:

$$T_{active} = T_{wu} + T_s + T_{proc} + T_{pd} + T_{backs}. \tag{9}$$

The wake-up T_{wu} and processing time duration T_{proc} depend on the microcontroller and can be found in the datasheet. Similarly, the duration T_s depends on the sensor units used for data measurement.

The preamble detector in the LoRa backscatter compares the preamble of incoming LoRa signals with stored chirps. Therefore, the duration of preamble detection depends on the length of the LoRa symbol. The duration of the LoRa preamble is given as [35]:

$$T_{Preamble} = (4.25 + NP) \cdot T_{Symbol} \tag{10}$$

where NP and T_{Symbol} are the number of preamble symbols and the duration of the LoRa symbol, respectively.

When the preamble detector detects LoRa, the LoRa backscatter tag waits for 2.25 symbol times to synchronize with the incoming LoRa packet and backscatter information data. After synchronization, the LoRa backscatter tag starts to encode the measured data bits into the payload part of the LoRa packet. Hence, the duration of the backscattering operation T_{backs} depends on the size of the LoRa payload.

The duration of the LoRa payload symbols can be calculated as :

$$T_{payload} = N_{payload} \cdot T_{Symbol}. \tag{11}$$

Where $N_{payload}$ is the number of payload symbols. T_{Symbol} is the period of the LoRa symbol. T_{Symbol} is defined as the time to send 2^{SF} chips. Since the bandwidth BW is equal to the chip rate, the symbol period is given as:

$$T_{Symbol} = \frac{2^{SF}}{BW}. \tag{12}$$

The number of payload symbols $N_{payload}$ is calculated using the equation 13 [35].

$$N_{Payload} = 8 + max\left(ceil\left(\frac{8 \cdot PL - 4 \cdot SF + 16 + 28 - 20 \cdot H}{SF - 2 \cdot DE}\right) \cdot \frac{1}{CR}, 0\right) \tag{13}$$

where ceil indicates the ceiling function, H represents the header with $H = 0$ when the header is enabled and $H = 1$ when no header is present, and DE is for the data rate with $DE = 1$ when the low data rate optimization is enabled and $DE = 0$ for the other case.

Physically, a LoRa transmission is not a stream of 1s and 0s bits. It is a continuous sequence of chirp waves that rapidly sweep up or down in frequency. To understand equation (13), let us take a look at the physical constraints of turning digital data into physical waves. Initially, the radio looks at your payload bytes (groups of 8 bits) and physically slices

your continuous data bitstream into blocks. If $SF = 7$, it cuts your data into 7-bit chunks. Each 7-bit chunk determines the exact starting frequency of a single physical radio chirp and represents a LoRa symbol. A LoRa transmission always starts with 8 unmodulated up-chirp symbols. This acts as a physical "wake up" signal, allowing the receiver's antenna to synchronize with the transmitter's frequency sweep [36]. The fraction $\frac{8 \cdot PL - 4 \cdot SF + 16 + 28 - 20 \cdot H}{4 \cdot (SF - 2 \cdot DE)}$ calculates how many blocks of data need to be sent. The equation multiplies your data bytes ($8 \cdot PL$) and subtracts overhead, while the denominator dictates how much physical data can fit onto a single symbol. Once the number of data words is computed, it is multiplied by $(CR + 4)$. This reflects the addition of forward error correction bits. If $CR = 1$, each word uses 5 chirps; if $CR = 3$, it uses 7, and so on [36]. Finally, since it is impossible to transmit a fraction of a chirp, the ceiling function rounds any fractional symbol numbers to the nearest whole integer [37].

We recall that each tag information bit has a duration of one LoRa symbol ($t_{bit} = T_{Symbol}$). As in [13], we exploit the idea that the maximum number of data bits that can be transmitted by a LoRa backscatter tag is equal to the number of LoRa payload symbols (i.e., each bit is transmitted within one LoRa symbol). And since $N_{payload}$ is fixed, the excess tag bits will wait for the detection of the next LoRa packet to be transmitted. This cycle will continue until the end of the transmission of all tag-measured bits.

We denote β as the number of LoRa packets required to transmit all tag bits, N_{data} as the number of tag bits to be transmitted, and then we can define α as:

$$\beta = ceil(\frac{N_{data}}{N_{payload}}). \tag{14}$$

Note that recent LoRa backscatter designs can encode multiple tag bits in one LoRa payload symbol [15] to increase throughput.

From equation (7)–(14), the average energy consumed by the LoRa backscatter sensor node to transmit N_{data} bits can be calculated as:

$$E_{cons} = \beta I_{av_s} \cdot V\,. \tag{15}$$

Where V is the voltage applied to the sensor node. The voltage applied to the sensor node can be chosen to be low to reduce the overall energy consumption of the node.

6.1.1 *Sensor node lifetime*

Now, we can calculate the theoretical lifetime of a battery-operated LoRa backscatter sensor node that performs sensing and backscatter communication using the following equation [38].

$$T_{lifetime} = \frac{B_{capacity}}{I_{av_s} + I_{discharge}} \tag{16}$$

where $B_{capacity}$ is the capacity of the battery (in mAh) and $I_{avaerage}$ is the battery self-discharge current.

6.2 *Multiple device energy model*

In general, a Backscatter system allows a single receiver to connect to multiple Backscatter devices. This increases the concurrency of devices accessing the wireless medium, as well as inter-tag interference, which increases energy consumption and hence reduces network lifetime. To address these issues, MAC (Media Access Control) protocols are used at the MAC layer, along with special signal processing techniques at the Physical layer. In LoRa backscatter,

interference between devices can be reduced using advanced tag design techniques [12, 14, 15]. For example, the authors in [15] generate a non-linear version of the LoRa chirp to improve concurrent transmission in the LoRa backscatter network. In [12], it was proposed to generate concurrent cyclic-shifted chirps across a distributed set of low-power devices in the network to increase concurrency in the LoRa backscatter system. The above two techniques require synthesizing the CSS type signal at the backscatter tag, which increases its complexity. However, The proposed energy model in this work considers a backscatter tag that receives a LoRa signal from a gateway to transmit data.

When multiple LoRa backscatter tags are transmitting simultaneously to the gateways, a collision will occur, resulting in packet retransmission.

We consider that the gateway leverages the time domain slotted ALOHA protocol to coordinate tags and minimize collisions, as in [18]. Each acknowledgment sent by the gateway is received and demodulated by all the sensors, but only the targeted tag will respond. Figure 5 shows an illustration of the operation of the MAC layer of the LoRa backscatter network. At first, each sensor node will randomly select a time slot and store it in its local counter. The gateway initiates the beginning of each slot by emitting a carrier signal. Upon detection of a gateway carrier signal, each node decreases the number of slots by one and transmits as soon as the number of slots reaches zero [18]. After receiving transmission from the sensor node, the gateway will send an acknowledgment to the node that experienced an error to retransmit the lost packet. To do so, the gateways broadcast a message that is received and demodulated by all the sensor nodes within the radio range, but only the target sensor node will respond. We assume that all sensor nodes are within the range of the gateway. Consequently, for each acknowledgment transmission, all the non-targeted nodes will consume an amount of energy for acknowledgment demodulation. This will increase the overall energy consumption of the nodes.

We assume that all LoRa backscatter tags have the same switching frequency and send packets on the same frequency channel. Thus, only the transmission time is random.

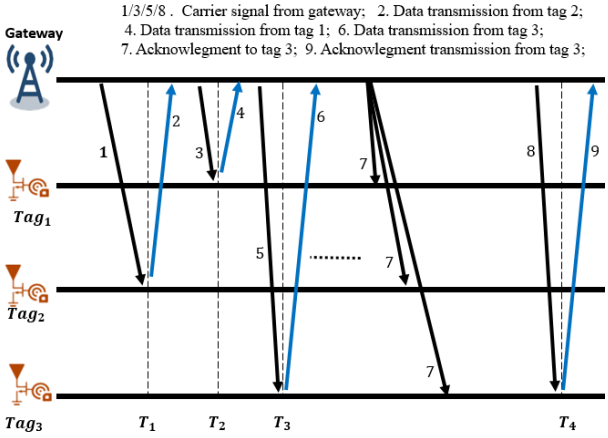


Figure 5. MAC layer protocol illustration

Table 3 presents the different states involved in multiple LoRa backscatter communications, along with their duration and current consumption.

When the sensor node wakes up (state 1) from sleep mode, it starts measuring the sensing parameters (state 2), and the microcontroller processes the measured data (state 3). Before transmission, the tag runs the ALOHA protocol and activates the preamble detector to detect the incoming LoRa packet as mentioned above (state 4). Upon detecting the LoRa packet, the tag waits for synchronization and starts encoding its bits in the LoRa payload part, then backscatters it back to the gateway(state 5). After transmitting its data, the LoRa backscatter tag enters idle mode for the duration T_{idl} (state 6) and starts receiving the acknowledgment from the gateway (state 7). T_{idl} represents the time between the end of the transmission and the beginning of the acknowledgment transmission. We choose its value to be 1s in this work. When it receives the acknowledgment, the tag processes it, and if an error occurs during transmission, the tag will prepare the

data for retransmission (state 8), retransmit it for a second time (state 9), and return to sleep mode (state 10). The time spent by the node during the acknowledgment reception can be given as

$$T_{rx} = (NP + 4.25 + N_{payload})T_{symbol}. \tag{17}$$

The average current consumption of the LoRa backscatter-based sensor node k for uplink (transmission) and downlink (reception) communication is given as follows:

$$I^k_{av_u d} = \beta \frac{1}{T_{cycle}} \sum_{i=1}^{N} T^k_i I^k_i \tag{18}$$

where N is the number of states involved in the operation of the sensor node k for the transmission of the uplink and downlink. T^k_i and I^k_i are the duration and current consumption in the state i of the sensor node k.

Downlink transmission involves all states encountered during the up-transmission phase (i.e., preamble detection and backscatter operation). The current consumption during downlink transmission can be obtained as:

$$I_{rt} = I_{pd} + I_{backs}. \tag{19}$$

Table 3. Different states in multiple battery-operated LoRa backscatter node communication with their current and duration of each

States	Description	Duration		Current consumption	
		Variable	Values	Variable	Values
1	Wake-up	T_{wu}	15μs	I_{wu}	10 μA/MHz [30]
2	Sensing	T_s	0.7ms	I_s	270 μA [31]
3	Processing	T_{proc}	4ms	I_{proc}	10 μA/MHz [30]
4	Preamble detection	T_{pd}	Equation (10)	I_{pd}	93.2 μW [16]
5	Backscatter	T_{backs}	Equation (11)	I_{backs}	Equation (6)
6	Idle mode	T_{idl}	1s	I_{idl}	6.4 μA
7	Receiving acknowledgment	T_{rx}	Equation (17)	I_{rx}	93.2 μW [16]
8	Prepare data for retransmission	T_{prep}	1ms	I_{prep}	19.6 μW
9	Retransmission	T_{rt}	T_{pd}+T_{backs}	I_{rt}	Equation (19)
10	Sleep	T_{sleep}	Equation (8)	I_{sleep}	2.9 μA [30]

6.2.1 *Collision and transmission error*

If packet generation in the network follows the Poisson distribution, the probability of no collision is derived as [39]:

$$p_{nco} = e^{-\alpha N_{LB} \rho_i \lambda T_{frame}} \tag{20}$$

where N_{LB} is the number of LoRa backscatter nodes in the network, ρ_i is the probability that the node will use SF_i, T_{frame} is the frame duration (The air time duration between the backscattered LoRa transmitter and the gateway), and λ is the

packet generation rate of the sensor node. α is the vulnerable time during which every LoRa backscatter is allowed to transmit data whenever it is available. Its value is 2 for unslotted ALOHA and 1 for slotted ALOHA. The frame duration is calculated as follows:

$$T_{frame} = T_{pd} + T_{payload}\,. \tag{21}$$

In LoRa backscatter, all sensor nodes share the excitation generated by the gateways; therefore, the probability that the node uses SF_i is equal to 1 ($SF_i = 1$). The packet generation rate is given as

$$\lambda = \frac{dc}{N_p T_{frame}} \tag{22}$$

where dc, N_p, and T_{bT} are the duty cycle and the number of packets in the node, respectively. N_p is equal to 1 for devices with limited-capacity [23].

The collision probability of data transmissions is given by

$$p_{collision} = 1 - p_{nco} = 1 - e^{-N_{LB}\lambda T_{frame}}. \tag{23}$$

In the proposed model, we consider the impact of bit errors due to non-ideal link quality. A closed-form of the physical layer BER of a LoRa backscatter system has been proposed in the literature [19, 40] and is given by:

$$p_e = 0.5 \sum_{q=1}^{n} u_q y_q^{-1.25} e^{-y_q} Q\left(1.28\sqrt{y_q \frac{E_b}{N_0}.N} - 1.28\sqrt{SF} + 0.4\right). \tag{24}$$

The probability that a transmitted data frame and acknowledgment is affected by at least one-bit error is given by [22].

$$pe_{data} = 1 - (1 - p_e)^{\frac{1}{CR}(N_{payload} - H_L)} \tag{25}$$

$$pe_{ack} = 1 - (1 - p_e)^{\frac{1}{CR}(N_{ack} - H_L)} \tag{26}$$

where H_L represents the size of the physical header.

Considering the collision, the probability of successful transmission of a data frame can be written as:

$$\begin{aligned} ps_{data} &= (1 - pe_{data})(1 - p_{collision}) \\ &= (1 - p_e)^{\frac{1}{CR}(N_{payload} - H)} e^{-N_{LB}\lambda T_{frame}} \end{aligned} \tag{27}$$

We assume that there is no collision for acknowledgment transmission. Similarly, the probability of successful acknowledgment transmission is given as:

$$ps_{ack} = 1 - pe_{ack}$$
$$= (1 - p_e)^{\frac{1}{CR}(N_{ack} - H)} \tag{28}$$

where N_{ack} is the length of the acknowledgment frame and is calculated as :

$$N_{ack} = 8 + max\left(ceil\left(\frac{8.PL_{ack} - 4.SF + 28 - 20.H}{SF - 2.DE}\right).\frac{1}{CR}, 0\right) \tag{29}$$

6.2.2 *Energy consumption for data transmission*

Now we consider the case where multiple nodes are deployed in the network. Each data transmission in LoRa backscatter comprises a preamble detection and backscatter. To model the energy consumption, we define the following possible situations after a sensor node transmits data, as illustrated in Figure 6(a)–(c).

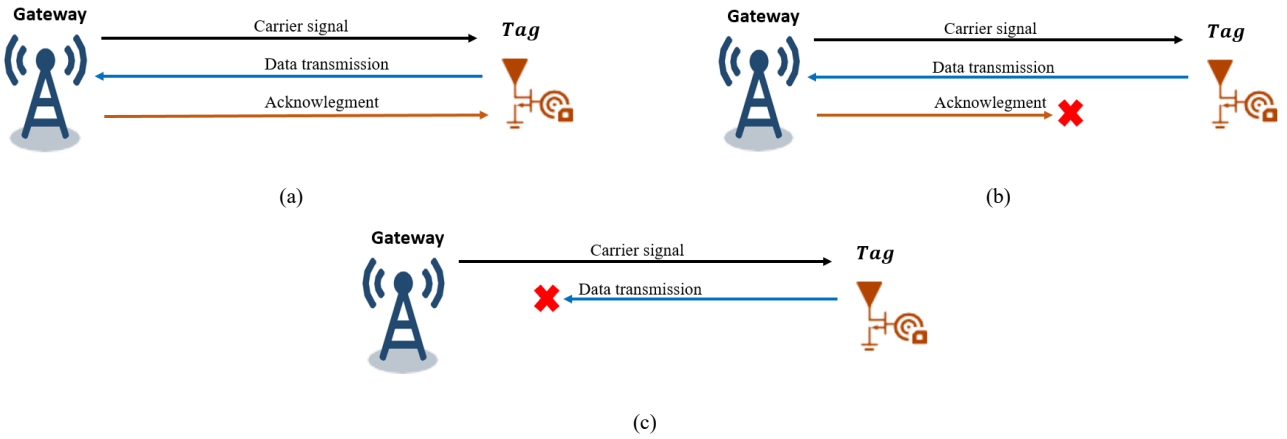


Figure 6. Illustration of the three possible scenarios. (a) The transmitted data is successfully received by the gateway in the first attempt and acknowledgment is received and demodulated by tag; (b) The transmitted data is successfully received by the gateway and acknowledgment is not received by tag; (c) The transmitted data is not successfully received by the gateway

1. **Case 1 (Successful transmission):** The transmitted data is successfully received by the gateways. An acknowledgment from the gateways is received and demodulated, and the node enters sleep mode until the next transmission.
2. **Case 2 (Failed transmission):** The transmitted data are successfully received by the gateways, but the acknowledgment is not received by the backscatter tag. The node will prepare for the retransmission of the lost packet. Retransmission attempts will continue until a successful transmission or the number of retransmissions is achieved after the node enters sleep mode until the next transmission.
3. **Case 3 (Failed transmission):** The transmitted data are not successfully received by the gateways, and the acknowledgment is not received by the backscatter tag. The node will prepare for the retransmission of the lost packet. Retransmission attempts will continue until a successful transmission or the number of retransmissions is achieved after the node enters sleep mode until the next transmission.

The energy consumption for the above three cases is given by:

$$E_1 = E_{pre} + E_{backs} + E_{idle} + E_{rx}$$

$$= P_{pre} \cdot T_{pre} + P_{backs} \cdot T_{backs} + P_{idle} \cdot T_{idle} + P_{rx} \cdot T_{rx} \tag{30}$$

$$E_2 = NR(E_{pre} + E_{backs} + E_{idle}) + E_{rx}$$

$$= NR(P_{pre} \cdot T_{pre} + P_{backs} \cdot T_{backs} + P_{idle} \cdot T_{idle} + P_{rx} \cdot T_{rx}) \tag{31}$$

$$E_3 = NR(E_{pre} + E_{backs} + E_{idle})$$

$$= NR(P_{pre} \cdot T_{pre} + P_{backs} \cdot T_{backs} + P_{idle} \cdot T_{idle}) \tag{32}$$

From equation (31), it can be seen that the preamble detection, backscatter, and idle state are repeated for each failed transmission.

We define the average total energy consumption for data transmission as follows.

$$E_{tot}^{avg} = \frac{E_1 \cdot ps_{data} \cdot ps_{ack} + E_2 \cdot ps_{data} \cdot (1 - ps_{ack}) + E_3 \cdot (1 - ps_{data})}{ps_{data} \cdot ps_{ack} + ps_{data} \cdot (1 - ps_{ack}) + (1 - ps_{data})}. \tag{33}$$

6.3 *Energy harvesting modeling*

Energy harvesting (EH) technology is seen as a promising environmentally friendly solution that extends the lifetime of these sensors and, in some cases, completely replaces the use of battery power [41]. In this paper, We consider the energy harvesting module proposed in [13]. The energy harvester proposed by the authors [13] is composed of three parts, i.e., a charger, a controller, and an output device; it consumes only 3.52 μW. The charger harvests and stores energy in the storage capacitor. The controller is used to manage the state transitions of the sensor node and prevent energy leakage caused by the remaining components. Finally, the outputter provides a voltage supply to activate and operate the sensing and backscatter communication to the gateway. The supply voltage is considered to be 3.3 V, and the minimum voltage is equal to 1.5 V. In this work,

To perform both energy harvesting and sensor data communication, a duty cycle is introduced, which defines the time interval used for both energy harvesting and sensor node communication. When a node is activated, the energy in the storage capacitor C_{ca} is continuously monitored by the power management module. If the stored energy in the capacitor is below the minimal threshold, the sensor node enters harvest mode and harvests energy from the ambient source. During the energy harvesting phase, the backscatter transmitter is put in an off state (i.e., sensing units, the preamble detector, the baseband processor, and the RF front-end are electrically isolated from the power source). When the energy in the storage capacitor exceeds the maximum threshold, the power management unit activates the backscatter transmitter for data communication. Given a capacitor value in farad, the equivalent energy is given as:

$$E = \frac{1}{2} C \cdot V^2 \tag{34}$$

where V is the supply voltage in volts.

We define the duty cycle as the percentage of the time the sensor node is in an ON state, and it is given as

$$d_{cycle} = \frac{T_{ON}}{T_{ON} + T_{OFF}} \tag{35}$$

where T_{ON} is the duration of the ON-state of the sensor node and T_{OFF} is the time interval for harvesting (charging and discharging the energy storage). The transmission time is affected by the value of C_{ca} [42]. To improve energy consumption efficiency, during the ON state, if the LoRa backscatter device still has enough energy after backscattering all its sensing data successfully, the microcontroller sends a message to the energy management module to enter harvest mode [13].

6.3.1 *System description*

1. Let $E(t)$ be the storage energy at a specific time instant.
2. Let E_H be the maximum energy threshold in the capacitor.
3. Let E_L be the minimum energy threshold in the capacitor.
4. We assume that the capacity of the battery is finite and equals to E_{ca}.
5. Let E_c be the consumed energy by the data communication.
6. Initially the device is in sleep mode. When the device wakes up, it consumes a constant amount of energy E_{wu}, followed by the sensing and processing energy consumption $E_{sensing}$ and E_{proc}, respectively. However, for simplicity, without loss of generality, we only consider energy consumption during the data communication phase E_c.
7. We denote E_r the remaining energy in the storage capacitor after data transmission.
8. At the beginning of each transmission, the device compares the stored energy in the battery at time instant t with the consumed energy. let's denote $E(T_k^-)$ as the energy stored before k^{th} transmission.

If $E(T_k^-) \leq E_c + E_L$, then the device is properly powered and the stored energy is sufficient for sensor communication.

If $E(T_k^-) < E_c + E_L$, the data communication process starts but, when the stored energy is detected to drop below E_L, the communication process is stopped leading to an unsuccessful transmission and an energy wastage of $E_c + E(T^-)$.

Figure 7 shows an illustration of the description of the system.

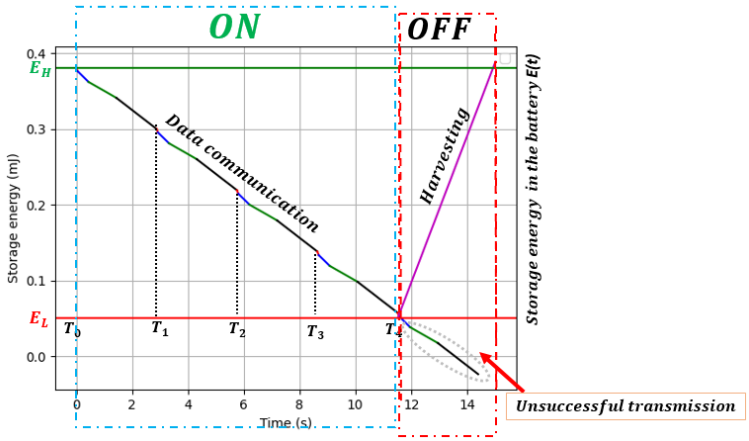


Figure 7. Illustration of the system description

We consider the case of a successful transmission, as illustrated in Figure 6(a). The different states involved in successful transmission are preamble detection, backscatter communication, idle state, and acknowledgment reception.

The energy harvested by the energy harvester is calculated as [43]:

$$E_{harvested} = \eta P_{harvester} \cdot G \cdot T_h \tag{36}$$

Where η is the energy conversion efficiency factor and G is the channel gain defined as:

$$G = \frac{\gamma}{D^2} \tag{37}$$

where γ is the channel parameter and depends on fading. D is the distance between the sensor node and the gateway.

7. Results and discussion

In this section, we will first analyze the current consumption of a LoRa backscatter-based sensor node and the lifetime for single-node communication with the LoRa gateways. Second, The energy consumption for data transmission in multiple node scenarios is analyzed, considering errors and collisions in the network. Finally, the energy harvesting-based sensor node is evaluated.

Table 4 summarizes the simulation parameters

Table 4. The simulation parameters

Parameters	Symbol	values
Bandwidth	BW (KHz)	125
Spreading factor	SF	9
Number of the preamble	NP	8
Data rate optimization enabled	DE	0
Header disabled	H	1
Coding rate	CR	4/5
Tag data size	Ndata_bytes	20
Supply voltage	V	3.3
Storage capacitor	C	70 mF

7.1 *Single node communication*

The current consumption and time spent in each state are given in Table 2 for single-node communication. Using the average current consumption defined in equation 15, We plot in Figure 8 the current consumption as a function of the node transmission cycle for different values of the LoRa payload. The tag payload size is set to 20 bytes ($N_{data} = 20$) bytes a typical payload in DR0 for the EU863-870 MHz Band [44]. It can be seen from the figure that the current consumption increases with the increase of the transmission cycle period. Specifically, for a sensor node that transmits every minute, the current consumption is about 0.24 μA compared to 0.05 μA for every transmission of five-minutes using the payload value of 59 bytes. Additionally, current consumption also decreases with increasing active LoRa payload. A payload of 10 bytes consumes 669 mA while transmitting every 2 mn compared to only 400 mA for a payload of 59 bytes. This is because the active LoRa payload has a direct effect on the transmission time.

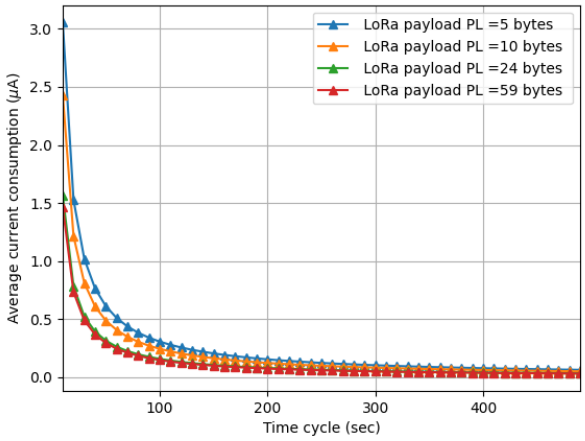


Figure 8. Average current consumption as a function of transmission cycle for different payload size PL

Figure 9 shows the evolution of the lifetime of the sensor node versus the transmission cycle for different tag payload sizes (N_{data}). The active LoRa payload size is set to 24 bytes. We can observe that the lifetime increases with the transmission cycle. A LoRa backscatter sensor node that transmits 20 bytes every 5 mn has a lifetime of about 14 years. When we decrease the transmission cycle to every 6 seconds, the lifetime drops to only 8 years, which can be translated to a reduction of about 57%. Additionally, transmitting a smaller tag data size yields a longer lifetime compared to a tag transmitting a higher data size.

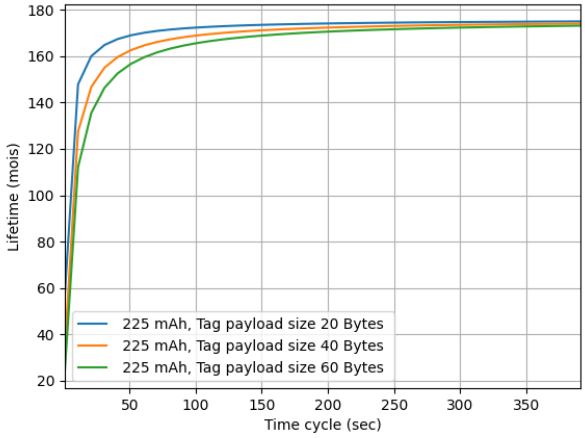


Figure 9. Sensor node lifetime versus the transmission cycle for different tag data sizes (N_{data})

7.2 *Multiple nodes communication*

When multiple nodes are deployed in the network, collisions will arise, increasing the total energy consumption of the sensor nodes and therefore limiting the performance of the network. Additionally, transmission errors due to link quality can lead to packet loss, which, in turn, translates to frequent packet retransmissions.

Figure 10 shows the evolution of the total energy consumption of a LoRa backscatter sensor as a function of the number of sensors in the network for different values of the duty cycle. The number of retransmissions is set to 5, and the tag payload is set to 20 bytes. We can observe that the total energy consumption increases with the number of LoRa backscatter sensors in the network. This is due to the increase in the probability of collisions and errors. For example,

the total energy increases from 60 μJ to 120 μJ when the number of nodes increases from 1 to 20. We can also observe saturation when the number of nodes exceeds 40.

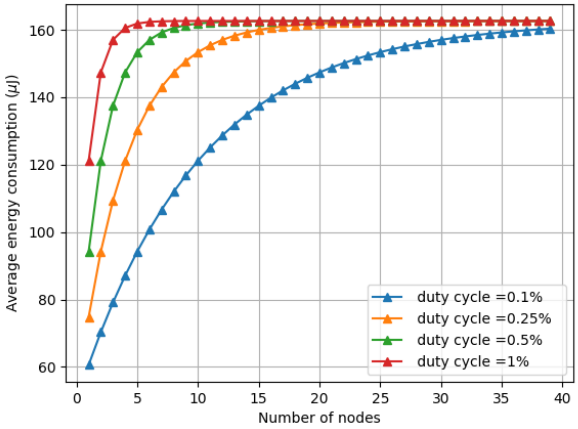


Figure 10. Total energy consumption as a function of the number of tags in the network for different duty cycles

Now we vary the number of retransmissions from 1, 3, 6, and 9 and analyze the effect of the number of nodes on total energy consumption. In Low-Power Wide-Area Networks (LPWANs) and short-range IoT protocols, the maximum number of retransmissions is typically capped at 1 to 3 attempts. Because battery life is highly prioritized, limiting retransmissions is essential to prevent rapid energy drain caused by keeping the radio transceiver awake to listen for acknowledgments [45]. However, in this simulation, we will increase the number of retransmissions to 9 to emphasize its effect. In Figure 11 it can be seen that the total energy increases with the number of retransmissions. For example, the total energy increases from 62 μJ to about 130 μJ when the number of retransmissions increases from 3 to 9. We can notice that there is a tradeoff between energy consumption and transmission reliability. In applications where interference levels are high, such as in residential buildings, a higher number of retransmissions can be chosen, resulting in better transmission reliability. Similarly, in low level interference applications, such as in environmental monitoring, the number of retransmissions can be considered to be low, resulting in better energy efficiency.

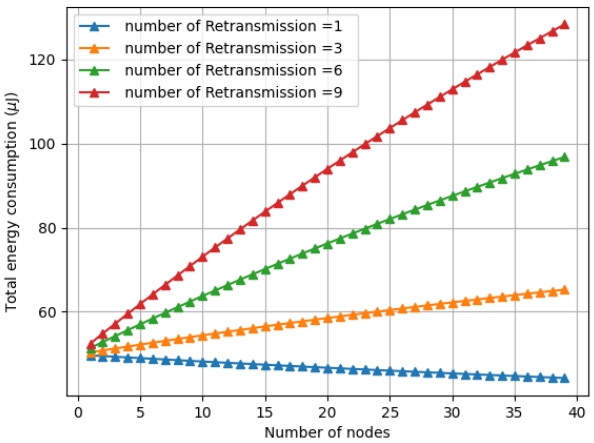


Figure 11. Total energy consumption as a function of the number of tags in the network for different Numbers of retransmission

The duty cycle also impacts total energy consumption. When the duty cycle increases from 0.1% to 1%, the energy consumption will increase from 93 μJ to 162 μJ, which is almost at the saturation of the duty cycle of 1%. This indicates that the duty cycle is an important factor to consider when deploying a LoRa backscatter sensor node to optimize network efficiency.

7.3 *Energy consumption for harvesting sensor node*

Now we power the node with an RF harvester. We consider the communication case where there is a successful transmission between the sensor node and the gateway (case 1) as shown in Figure 6(a). We assume the distance from the source to the tag to be 3 m. Figure 12 shows the evolution of the storage energy as a function of time during data communication. As can be seen, The storage energy, initially full, starts to drop from the maximum threshold toward the minimal threshold as the communication phase begins. The LoRa backscatter first starts the preamble detection, which has a duration of 50 ms and consumes 46 μJ, and backscatters the data to the gateway, which spends 390 ms and consumes 14 mJ. After backscattering the data, the tag will enter idle mode for a duration of 1 ms and consume 21 mJ, then starts receiving the acknowledgment from the gateway, which has a duration of 1.44 s and consumes 41 mJ. We can notice that the remaining energy after data communication is higher than the minimal energy threshold. Therefore, multiple data transmissions are possible during the ON state.

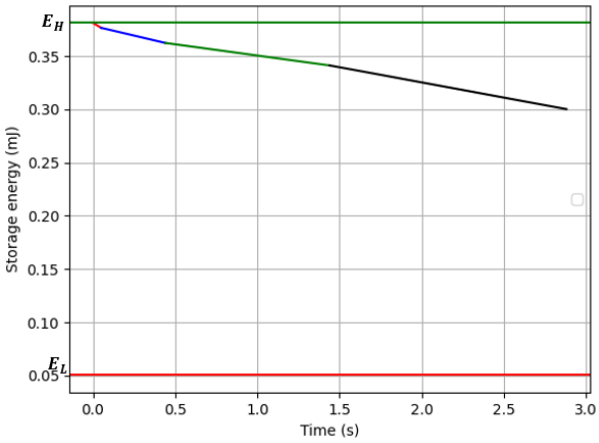
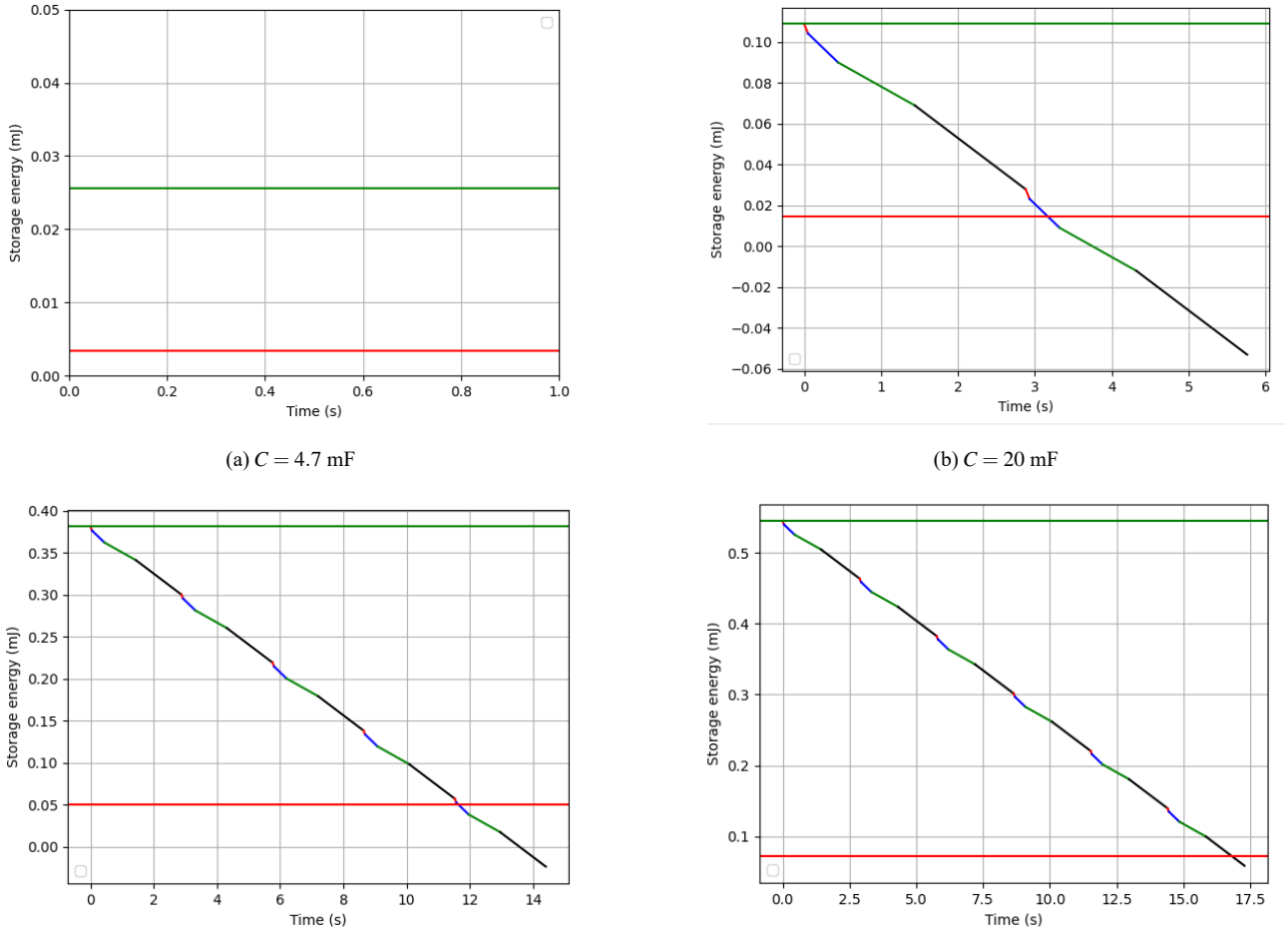


Figure 12. Evoluation of the storage energy during data communication for a capacity $C = 70$ mF

Figure 13 shows the evolution of the number of possible data transmissions within an ON state for different values of the storage capacitor.

For a capacitor value of 4.7 mF, the difference between the maximum and minimum energy thresholds is less than the energy consumed during data communication. Therefore, no transmission is initiated, as shown in Figure 13(a). There are two alternatives in this case. The first solution consists of increasing the storage capacitor value, and the second alternative consists of choosing optimal values of active LoRa parameters, such as the spreading factor, the coding rate, and the payload size, to decrease the transmission time. When we increase the storage capacitor values to 20 mF, 70 mF, and 100 mF the data transmission starts, meaning that the accumulated energy in the storage capacitor is higher than the consumed energy. The number of data transmissions varies according to the values of the storage capacitor. Specifically, The number of data transmissions possible for a capacitor value of 20 mF is equal to 1, as shown in Figure 13(b), and it increases to 4 and 5 for capacitor values of 70 mF and 100 mF, as shown in Figure 13(c) and 13(d), respectively.



(a) $C = 4.7$ mF

(b) $C = 20$ mF

(c) $C = 70$ mF

(d) $C = 100$ mF

Figure 13. The number of possible data transmissions in an ON state for different values of capacitor

8. Discussion

Many published works focus on the development of energy models for wireless communication protocols, considering that many IoT devices are expected to run on constrained energy sources [22, 38, 46]. In [46], a detailed and comprehensive analytical model of Sigfox device current consumption, lifetime, and energy cost of data delivery has been proposed. The model takes into consideration the real behavior of Sigfox device hardware, the different communication settings and mechanisms (uplink/downlink communication, payload size, and uplink bit rate), and the impact of frame losses. The evaluation results of the proposed model show that, using a Sigfox device powered by a 2400 mAh battery, a theoretical lifetime of 1.5 or 2.5 years can be achieved while sending one message every 10 min at 100 bit/s or 600 bit /s, respectively, and an asymptotic lifetime of 14.6 years as the message transmission rate decreases. The authors also considered an alternative energy harvesting source and evaluated the minimum feasible transaction period for a Sigfox device powered by an energy harvesting source. The current consumption model, lifetime, and energy cost per bit delivered by a battery-operated Bluetooth Mesh sensor node are presented in [38]. Through evaluation, they found that a sensor device running on a simple 235 mAh battery and sending a data message every 10 seconds can achieve a lifetime of up to 15.6 months. The authors do not account for the energy cost of frame losses and packet retransmission in their model. In [22], an analytical model is presented to allow the characterization of LoRaWAN end-device current consumption, lifetime, and energy cost of data bits. The evaluation results show that a well-configured LoRaWAN end-device platform powered by

a 2400 mAh battery can achieve a 1-year lifetime while sending one message every 5 min, and an asymptotic theoretical lifetime of 6 years for infrequent communication. The proposed energy model includes mechanisms of the MAC layer, such as acknowledgment, receiving windows, and retransmissions.

Our energy consumption model is based on the LoRa backscatter communication principle, which is detailed further in Section 6.1. The model relies on the theoretical current consumption values provided in the datasheet to estimate the energy consumption of the LoRa backscatter-based sensor node. However, it is also possible to develop a prototype LoRa backscatter sensor node and measure practical energy consumption values in each state through experimentation [6, 15], which is left as a future research direction.

Our proposed energy model also includes the mechanisms of the MAC layer, such as the use of acknowledgments and retransmissions.

9. Limitation

Our energy consumption model is based on the principle of transmitting one tag bit in every LoRa symbol [13], which limits its applicability. Recent LoRa backscatter systems can encode multiple tag data within one LoRa symbol and extend communication throughput [15].

Furthermore, our proposed model is based on the assumption that the backscatter tag receives a LoRa signal as excitation, which the tag uses to generate a LoRa compatible signal. However, in some backscatter designs, the backscatter tag receives a continuous wave signal and synthesizes LoRa compatible packets [4, 6, 19, 47] that consume more power, hence increasing the overall power consumption of LoRa backscatter systems.

In addition, this model is based on the theoretical values provided by the datasheet or experiments from the literature. A realistic analysis, i.e., a model derived from measurements performed on real LoRa backscatter devices, is crucial to validate the theoretical values.

In future research, the authors plan to implement real prototypes to validate the theoretical and simulation data obtained in this work. We will implement end-to-end LoRaWAN communication between a LoRa backscatter sensor node and a network server. Using a current analyzer, we measure the current consumed in the sensing, preamble detection, backscatter, and sleep states. The current analyzer is configured to trigger when the current spikes above a specific threshold [48] to capture the entire transmission sequence (Wake-up → detection → processing → preamble detection → backscatter communication → sleep).

10. Conclusion and future work

In this paper, the energy consumption of a full-duplex LoRa backscatter-based sensor node is modeled. The derived model is divided into three parts. First, we developed the energy consumption model for a battery-operated sensor node that transmits sensor data to the gateway only in the uplink direction. The experiment shows that the current consumption decreases with a decrease in the transmission cycle. Additionally, with a battery capacity of 225 mAh, a LoRa backscatter sensor node that transmits 20 bytes every 5 minutes has a lifetime of about 14 years. Second, we have extended the model to account for the energy cost during the acknowledgment transmission in full-duplex communication (uplink and downlink). The energy cost in full-duplex communication depends on the error probability and the collision probability, as well as the number of possible retransmissions. Both the error probability and the collision probability vary with the number of nodes in the network and consequently the total energy consumption. Specifically, the simulation result shows that the total energy increases from 60 μJ to 120 μJ when the number of nodes increases from 1 to 20. Finally, we develop an energy harvesting model for a LoRa backscatter sensor that communicates using an ambient energy source. The results show that the number of possible communications during the ON state depends on both active LoRa parameters, such as the spreading factor, coding, and payload size, and the value of the storage capacitor.

Abbreviation

MCU	Micro-Controller Unit
IoT	Internet of Things
WSNs	Wireless Sensor Networks
LoRa	Long Range
LPWAN	Low Power Wide Area Network
LoRaWAN	LoRa Wide Area Network
BLE	Bluetooth Low Energy
RF	Radio Frequency
BPSK	Binary Phase Shift Keying
OOK	On Off Keying
FSK	Frequency Shift Keying
SF	Spreading Factor
CR	Coding Rate
EH	Energy Harvesting
DR	Data Rate
PL	Payload
NP	Number of Preamble
ToA	Time on Air
BW	Bandwidth
CSS	Chirp Spread Spectrum
CW	Continuous Wave
CRC	Cyclic Redundancy Check

Author Contributions

Siaka Konaté: Writing—review & editing, Writing—original draft, Visualization, Software, Methodology, Investigation, Formal analysis, Conceptualization. Changli Li: Writing—review & editing, Supervision, Methodology. Drissa Traoré: Writing—review & editing, Supervision, Methodology. Diouba Sacko: Writing—review & editing, Supervision, Methodology. Souleymane Coulibaly: Writing—review & editing, Methodology.

Data Availability Statement

No data was used for the research described in the article.

Funding

This work was funded by the National Natural Science Foundation of China under Grant No 61871174.

Conflicts of Interest

The authors declare the following financial interests/personal rela tionships which may be considered as potential competing interests: Changli Li reports financial support was provided by National Natural Science Foundation of China. If there are other authors, they declare that they have no known competing financial interests or personal relationships that could have appeared to influence the work reported in this paper.

References

[1] Statista, "Internet of Things (IoT) connected devices installed base worldwide from 2015 to 2025 (in billions)," [online]. Available: https://www.statista.com/statistics/471264/iot-number-of-connected-devices-worldwide/. [Accessed Feb. 5, 2026].

[2] P. V. Dudhe, N. V. Kadam, R. M. Hushangabade, and M. S. Deshmukh, "Internet of things (IOT): An overview and its applications," In *Proc. 2017 International Conference on Energy, Communication, Data Analytics and Soft Computing*, 2017, pp. 2650–2653.

[3] A. Gupta, T. Gulati, and A. K. Bindal, "WSNs based IoT applications: A review," In *Proc. 2022 10th International Conference on Emerging Trends in Engineering and Technology-Signal and Information Processing*, 2022, pp. 1–6.

[4] M. Katanbaf, A. Weinand, and V. Talla, "Simplifying backscatter deployment: Full-duplex LoRa backscatter," In *Proc. 18th USENIX Symposium on Networked Systems Design and Implementation*, 2021, pp. 955–972.

[5] S. Konate, C. Li, and L. Xu, "LoRa backscatter automated irrigation approach: Reviewing and proposed system," In *Proc. 2020 6th International Conference on Robotics and Artificial Intelligence*, 2020, pp. 205–213.

[6] V. Talla, M. Hessar, B. Kellogg, A. Najafi, J. R. Smith, and S. Gollakota, "LoRa backscatter: Enabling the vision of ubiquitous connectivity," *Proceedings of the ACM on Interactive, Mobile, Wearable and Ubiquitous Technologies*, vol. 1, no. 3, 2017.

[7] A. Lazaro, M. Lazaro, and R. Villarino, "Room-level localization system based on LoRa backscatters," *IEEE Access*, vol. 9, pp. 16004–16018, 2021.

[8] J. Jiang, J. Wang, Y. Chen, Y. Liu, and Y. Liu, "LocRa: Enable practical long-range backscatter localization for low-cost tags," In *Proc. 21st Annual International Conference on Mobile Systems, Applications and Services*, 2023, pp. 317–329.

[9] S. Zhang, W. Wang, N. Zhang, and T. Jiang, "LoRa backscatter assisted state estimator for micro aerial vehicles with online initialization," *IEEE Transactions on Mobile Computing*, vol. 21, no. 11, pp. 4038–4050, 2022.

[10] M. Lazaro, A. Lazaro, R. Villarino, and D. Girbau, "Smart mask for temperature monitoring with LoRa backscattering communication," In *Proc. 2021 6th International Conference on Smart and Sustainable Technologies*, 2021, pp. 1–4.

[11] H. Jiang, J. Zhang, X. Guo, and Y. He, "Sense me on the ride: Accurate mobile sensing over a LoRa backscatter channel," In *Proc. 19th ACM Conference on Embedded Networked Sensor Systems*, 2021, pp. 125–137.

[12] M. Hessar, A. Najafi, and S. Gollakota, "NetScatter: Enabling large-scale backscatter networks," In *Proc. 16th USENIX Symposium on Networked Systems Design and Implementation*, 2019, pp. 271–284.

[13] Y. Peng, L. Shangguan, Y. Hu, Y. Qian, X. Lin, X. Chen, et al., "PLoRa: A passive long-range data network from ambient LoRa transmissions," In *Proc. ACM SIGCOMM 2018 Conference*, 2018, pp. 147–160.

[14] J. Jiang, Z. Xu, F. Dang, and J. Wang, "Long-range ambient LoRa backscatter with parallel decoding," In *Proc. 27th Annual International Conference on Mobile Computing and Networking*, 2021. pp. 684–696.

[15] Y. Ren, P. Cai, J. Jiang, J. Du, and Z. Cao, "Prism: High-throughput LoRa backscatter with non-linear chirps," In *Proc. IEEE INFOCOM 2023-IEEE Conference on Computer Communications*, 2023, pp. 1–10.

[16] X. Guo, L. Shangguan, Y. He, J. Zhang, H. Jiang, and A. A. Siddiqi, "Efficient ambient LoRa backscatter with on-off keying modulation," *IEEE/ACM Transactions on Networking*, vol. 30, no. 2, pp. 1–14, 2021.

[17] H. Li, X. Tong, Q. Li, and X. Tian, "XORLoRa: LoRa backscatter communication with commodity devices," In *Proc. 2020 IEEE 6th International Conference on Computer and Communications*, 2020, pp. 706–711.

[18] X. Guo, Y. He, N. Jing, J. Zhang, H. Jiang, and Y. Liu, "Saiyan: Design and implementation of a low-power demodulator for LoRa backscatter systems," In *Proc. 19th USENIX Symposium on Networked Systems Design and Implementation*, 2022, pp. 437–451.

[19] G. Lin, A. Elzanaty, and M. S. Alouini, "LoRa backscatter communications: Temporal, spectral, and error performance analysis," *IEEE Internet of Things Journal*, vol. 10, no. 18, pp. 16412–16426, 2023.

[20] A. S. Ali, L. Bariah, S. Muhaidat, P. Sofotasios, and M. Al-Qutayri, "Performance analysis of LoRa-backscatter communication system in AWGN channels," In *Proc. 2021 4th International Conference on Advanced Communication Technologies and Networking*, 2021, pp. 1–5.

[21] S. Konate, C. Li, and L. Xu, "Theoretical evaluation of the performance of ambient LoRa backscatter communication," In *Proc. Fifteenth International Conference on Machine Vision*, Rome, Italy, 2023, vol. 12701, p. 41.

[22] L. Casals, B. Mir, R. Vidal, and C. Gomez, "Modeling the energy performance of LoRaWAN," *Sensors*, vol. 17, no. 10, p. 2364, 2017.
[23] S. Maudet, G. Andrieux, R. Chevillon, and J. F. Diouris, "Refined node energy consumption modeling in a LoRaWAN network," *Sensors*, vol. 21, no. 19, p. 6398, 2021.
[24] Semtech, "Lora modulation basics semtech," Semtech, 2015. [online]. Available: https://procon.bg/article/semtech-an120022-lora-modulation-basics. [Accessed Feb. 5, 2026].
[25] LoRa Alliance, "LoRa," 2015. [online]. Available: https://lora-alliance.org/. [Accessed Feb. 5, 2026].
[26] K. Mekki, E. Bajic, F. Chaxel, and F. Meyer, "A comparative study of LPWAN technologies for large-scale IoT deployment," *ICT Express*, vol. 5, no. 1, pp. 1–7, 2019.
[27] H. Mroue, A. Nasser, B. Parrein, S. Hamrioui, E. Mona-Cruz, and G. Rouyer, "Analytical and simulation study for LoRa modulation," In *Proc. 2018 25th International Conference on Telecommunications*, 2018, pp. 655–659.
[28] J. D. Griffin and G. D. Durgin, "Complete link budgets for backscatter-radio and RFID systems," *IEEE Antennas and Propagation Magazine*, vol. 51, no. 2, pp. 11–25, 2009.
[29] T. Bouguera, J. F. Diouris, J. J. Chaillout, R. Jaouadi, and G. Andrieux, "Energy consumption model for sensor nodes based on LoRa and LoRaWAN," *Sensors*, vol. 18, no. 7, p. 2104, 2018.
[30] Ambiqmicro, "Apollo2 MCU datasheet," 2017. [online]. Available: https://ambiq.com/wp-content/uploads/2020/08/Apollo-MCU-Datasheet.pdf. [Accessed Oct. 6, 2025].
[31] Sensirion, "Datasheet SHTC3: Humidity and temperature sensor IC," 2022. [online]. Available: https://sensirion.com/media/documents/643F9C8E/63A5A436/Datasheet_SHTC3.pdf. [Accessed Oct. 6, 2025].
[32] Analog Devices, "ADG901/ADG902: 0 Hz to 4.5 GHz, 40 dB off isolation at 1 GHz, 17 dBm P1dB at 1 GHz SPST switches," 2016. [online]. Available: https://www.analog.com/media/en/technical-documentation/data-sheets/adg901_902.pdf. [Accessed Sep. 30, 2025].
[33] A. Varshney, L. Harms, C. Pérez-Penichet, C. Rohner, F. Hermans, and T. Voigt, "LoRea: A backscatter reader for everyone!", 2016, arXiv:1611.00096.
[34] Texas Instruments, "MSP430FR5969," [online]. Available: https://www.ti.com/product/MSP430FR5969. [Accessed Sep. 30, 2025].
[35] Semtech, "LoRa design guide," 2013. [online]. Available: https://www.semtech.com/uploads/technology/LoRa/lora-and-lorawan.pdf. [Accessed May 28, 2025].
[36] F. Busacca, S. Mangione, S. Palazzo, F. Restuccia, and I. Tinnirello, "SDR-LoRa, an open-source, full-fledged implementation of LoRa on software-defined-radios: Design and potential exploitation," *Computer Networks*, vol. 241, p. 110194, 2024.
[37] Z. Xu, S. Tong, P. Xie, and J. Wang, "From demodulation to decoding: Toward complete LoRa PHY understanding and implementation," *ACM Transactions on Sensor Networks*, vol. 18, no. 4, 2023.
[38] S. M. Darroudi, R. Caldera-Sánchez, and C. Gomez, "Bluetooth mesh energy consumption: A model," *Sensors*, vol. 19, no. 5, 2019. https://doi.org/10.3390/s19051238.
[39] M. A. A. Khan, H. Ma, S. M. Aamir, and Y. Jin, "Optimizing the performance of pure ALOHA for LoRa-based ESL," *Sensors*, vol. 21, no. 15, 2021.
[40] A. S. Ali, L. Bariah, S. Muhaidat, P. C. Sofotasios, and M. Al-Qutayri, "On the performance of LoRa-enabled backscatter communication," TechRxiv, 2022. [Online]. Available: https://doi.org/10.36227/techrxiv.21641144.v1. [Accessed Aug. 3, 2026].
[41] T. Sanislav, G. D. Mois, S. Zeadally, and S. C. Folea, "Energy harvesting techniques for Internet of Things (IoT)," *IEEE Access*, vol. 9, pp. 39530–39549, 2021.
[42] C. Konstantopoulos, E. Koutroulis, N. Mitianoudis, and A. Bletsas, "Converting a plant to a battery and wireless sensor with scatter radio and ultra-low cost," *IEEE Transactions on Instrumentation and Measurement*, vol. 65, no. 2, pp. 388–398, 2016.
[43] F. Sangoleye, N. Irtija, and E. E. Tsiropoulou, "Smart energy harvesting for Internet of Things networks," *Sensors*, vol. 21, no. 8, 2021.
[44] The Things Network, "LoRaWAN regional parameters - EU868," [online]. Available: https://www.thethingsnetwork.org/docs/lorawan/regional-parameters/eu868/. [Accessed May 28, 2025].
[45] S. N. Jafari and B. M. C. Silva, "A hybrid energy-aware communication protocol for data size and channel throughput adaptation in rural IoT networks," *Internet of Things*, vol. 37, p. 101944, 2026.

[46] C. Gomez, J. C. Veras, R. Vidal, L. Casals, and J. Paradells, "A Sigfox energy consumption model," *Sensors*, vol. 19, no. 3, 2019.

[47] D. Belo, R. Correia, Y. Ding, S. N. Daskalakis, G. Goussetis, and A. Georgiadis, "IQ impedance modulator front-end for low-power LoRa backscattering devices," *IEEE Transactions on Microwave Theory and Techniques*, vol. 67, no. 12, pp. 5307–5314, 2019.

[48] M. Asad Ullah, K. Mikhaylov, and H. Alves, "Experiment-based models for air time and current consumption of LoRaWAN LR-FHSS," *IEEE Internet of Things Journal*, vol. 12, no. 24, pp. 52621–52631, 2025.